

Biexciton formation in $\text{Cd}_x\text{Zn}_{1-x}\text{Se}/\text{ZnSe}$ quantum-dot and quantum-well structures

K. Herz, T. Kümmell, G. Bacher, and A. Forchel

Technische Physik, Universität Würzburg, D-97074 Würzburg, Germany

B. Jobst,* D. Hommel,* and G. Landwehr

Experimentelle Physik III, Universität Würzburg, D-97074 Würzburg, Germany

(Received 31 July 1997)

The dimensionality dependence of the biexciton formation process is investigated by comparing $(\text{Cd,Zn})\text{Se}/\text{ZnSe}$ quantum-dot and quantum-well structures using time-resolved photoluminescence (PL) spectroscopy. Modeling the onset of the biexciton PL signal with a system of rate equations, we obtain a biexciton formation coefficient of about $4 \times 10^{-10} \text{ cm}^2/\text{ps}$ for 35-nm quantum dots and of $0.2 \times 10^{-10} \text{ cm}^2/\text{ps}$ for the quantum-well reference, respectively, indicating a distinct enhancement of the biexciton formation efficiency in quantum dots. By analyzing the spectral line shape of the PL signal, an increase of the biexciton binding energy from 6.4 meV in the case of the quantum-well reference, to 11.3 meV for the quantum dots, is determined. [S0163-1829(97)04747-4]

A variety of recent publications were related to the optical properties of excitonic molecules (biexcitons) in quasi-two-dimensional semiconductor heterostructures.¹⁻⁶ Compared to the bulk, an increased contribution of the biexciton transition to the photoluminescence (PL) line shape is observed for quantum wells (QW's).⁶ In addition, an enhancement of the biexciton binding energy (BBE) has been found by reducing the dimension from bulk material to quasi-two-dimensional structures, which is a consequence of the increased Coulomb interaction due to carrier confinement.^{1,6} This effect is even more important for totally confined systems like quantum dots (QD's).⁷⁻¹²

In contrast to various studies on the BBE, experimental and theoretical results related to the biexciton formation dynamics in semiconductor nanostructures are still rare. In QW's an increased biexciton formation efficiency is found by analyzing the biexciton formation process for a resonant generation of cold^{5,13} or localized excitons.³ This was explained by the small center of mass kinetic energy in the quantum-well layer characterizing these exciton states. Due to the three-dimensional carrier confinement, the lateral exciton migration is completely suppressed in QD's, which might enhance the biexciton formation efficiency. However, up to now, a direct comparison of the biexciton formation process in QD's and QW's is still lacking.

In this paper, we compare the biexciton formation process and the PL line shape of $(\text{Cd,Zn})\text{Se}/\text{ZnSe}$ QD's and QW's. The biexciton formation coefficient is determined by evaluating the onset of the biexciton PL signal after pulsed excitation. Applying a straightforward line shape analysis, the dimensionality dependence of the BBE is obtained.

The $\text{Cd}_{0.12}\text{Zn}_{0.88}\text{Se}/\text{ZnSe}$ quantum-well heterostructure under investigation was grown by molecular-beam epitaxy on a (100)-oriented undoped GaAs substrate using a 200-nm GaAs buffer layer. The $L_z = 5 \text{ nm}$ QW is cladded between a 20-nm ZnSe top barrier layer and a 70-nm buffer layer. The sample is fully strained, with an in-plane lattice constant of the GaAs substrate. A dot pattern consisting of a large array ($800 \times 800 \mu\text{m}^2$) of individual dots was defined in a poly-

methmethacrylate resist by electron-beam lithography, and transferred into the semiconductor by a wet chemical etching process using a $\text{K}_2\text{Cr}_2\text{O}_7:\text{HBr}:\text{H}_2\text{O}$ solution. This technique was used to fabricate QD's of high optical quality with a lateral extension $L_x = 35 \text{ nm}$.¹⁴ The quasi-zero-dimensional behavior of such a structure is confirmed by a systematic size-dependent blueshift of the PL signal with decreasing dot diameter.¹⁴ Because the same QW layer is used for two-dimensional (2D) and zero-dimensional (0D) systems, a direct comparison of quasi-two-dimensional and quasi-zero-dimensional excitons and biexcitons is possible.

In order to study the biexciton formation dynamics in the QW and QD structures, time-resolved PL spectroscopy is used. Sample excitation was performed at a temperature of 2 K by a pulsed frequency-doubled titanium sapphire laser, yielding pulses with a pulse length of 1.5 ps and a repetition rate of about 82 MHz. The PL signal was dispersed by a 0.32-m Jobin Yvon monochromator, and recorded using a Streak camera with an S20 cathode and a subsequent charge coupled device array. The overall time resolution of the setup is about 5 ps.

In Fig. 1, a set of time-integrated PL spectra after pulsed excitation is shown for the unpatterned QW sample (a) and the QD's (b) for average excitation densities P ranging from 1 to $100 \text{ W}/\text{cm}^2$. The excitation was performed in the CdZnSe layer with an excess energy of about one LO-phonon energy in order to avoid carrier capture from the barrier layer, and to guarantee an efficient and fast occupation of the exciton ground state.¹⁵

In order to compare the line shape, the PL spectra are normalized to the peak exciton intensity. Below an excitation density of $1 \text{ W}/\text{cm}^2$, the spectra of the QD and the QW sample consist of a single line which is attributed to the radiative recombination of the heavy-hole exciton. For higher excitation intensities, a second peak appears energetically below the exciton luminescence, which increases in intensity superlinearly with the excitation density, and which is attributed to the recombination of biexcitons. Comparing PL spectra at the same excitation power, the biexciton con-

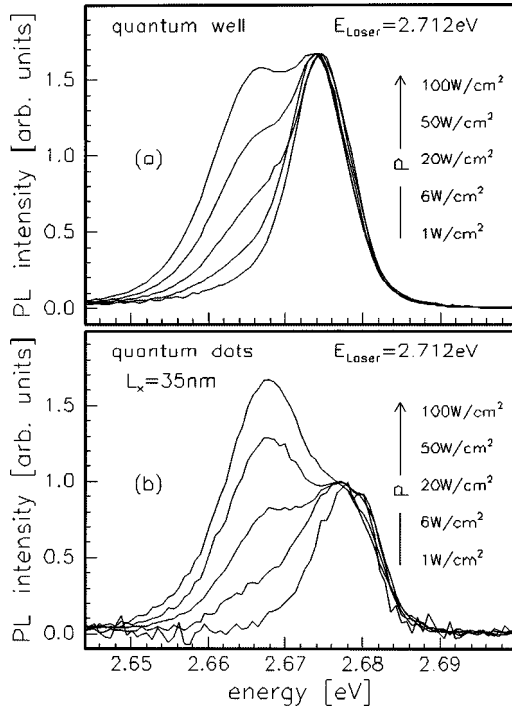


FIG. 1. Normalized PL spectra of the unpatterned quantum-well reference (a) and the 35-nm dot array (b) for different excitation densities P at $T=2$ K.

tribution is much stronger in the case of QD's, indicating a higher biexciton formation efficiency. In addition, the energetic spacing between exciton and biexciton peaks is significantly increased.

Quantitative information about the biexciton formation efficiency in QD's and the QW is obtained by evaluating the transient onset of the biexciton PL signal. In Fig. 2 the biexciton PL intensity of the QD's and the QW is plotted versus time for an average excitation density of 100 W/cm^2 . In the case of the QW the PL maximum of the biexciton signal is reached after 50 ps, while for QD's a significantly faster onset of the biexciton peak is obtained.

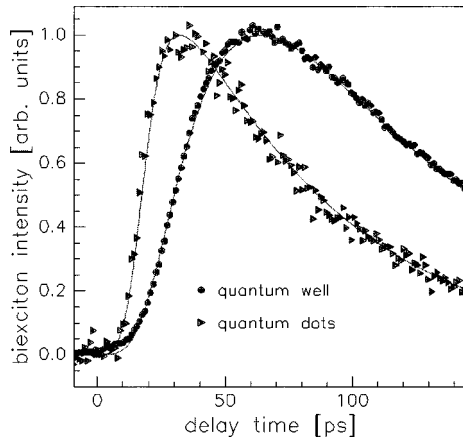


FIG. 2. Normalized PL intensity of the biexciton signal of 35-nm quantum dots (triangles) and the unpatterned quantum well (circles) as a function of time for an excitation density of 100 W/cm^2 . The solid lines represent best fits according to Eqs. (1) and (2).

In order to obtain the biexciton formation coefficient quantitatively, we have to analyze the onset of the biexciton PL intensity in more detail. Following Ref. 16, a straightforward kinetic theory was applied, using the following rate equations to describe a system of excitons and biexcitons with densities n_x and n_b :

$$\frac{dn_x}{dt} = G(t) - \frac{n_x}{\tau_x} + \frac{n_b}{\tau_b} - 2Cn_x^2, \quad (1)$$

$$\frac{dn_b}{dt} = -\frac{n_b}{\tau_b} + Cn_x^2, \quad (2)$$

where τ_x and τ_b are the exciton and the biexciton lifetimes, respectively, and C is the biexciton formation coefficient. The generation rate of excitons $G(t)$ takes into account the finite relaxation time of the photogenerated carriers into the exciton ground state, as determined by evaluating the transient onset of the exciton PL signal. The thermal dissociation of biexcitons into excitons is neglected, which is a rather good assumption for the low temperature of 2 K and the high BBE in wide-gap II-VI nanostructures. The above rate equations were solved numerically, and the resulting time transients of the exciton and the biexciton luminescence signal were compared to the experimental data, taking into account the finite time resolution of the setup. In order to obtain the biexciton formation coefficient C quantitatively, the exciton peak density generated by the laser pulse has to be determined very accurately, as described in Ref. 3. In a first approximation the same density of photogenerated carriers was assumed for the QD's and the QW sample.

In Fig. 2 the experimental data (circles, triangles) are compared to the model calculations (solid lines). A biexciton formation coefficient of $C = 0.2 \times 10^{-10} \text{ cm}^2/\text{ps}$ is obtained for the QW. In contrast, $C = 4 \times 10^{-10} \text{ cm}^2/\text{ps}$ is determined for QD's, which is more than one magnitude higher than the value for the QW, indicating a significantly enhanced biexciton formation efficiency in QD's. The transition from QW to QD corresponds to a change from a system allowing lateral exciton migration to a totally confined system. Thus the reduction of dimensionality results in a more efficient biexciton formation. This is in qualitative agreement with data published by R. Spiegel *et al.*,³ who reported an enhancement of C in QW's caused by a suppression of lateral exciton migration due to localization effects.

In order to estimate the BBE, a line shape analysis has to be performed. In the case of the QW we can follow Phillips *et al.*,¹³ and determine the BBE using a model line shape of thermally distributed biexcitons, and taking into account an inhomogeneous line broadening due to well width and alloy fluctuations. In Fig. 3(a) we compare this model line shape and the experimental data for the QW for an average excitation density of 100 W/cm^2 . In addition, the contributions of biexcitons and excitons are plotted separately as dashed lines, where the latter is deduced from the PL signal at low excitation densities. A good agreement between experimental data and model calculations can be achieved, yielding a BBE of 6.4 meV in the 2D sample. It has to be noted that this value should be regarded as a lower limit. Taking into account the localization of excitons and biexcitons a low temperatures,⁴ a Gaussian fit for the biexciton line shape in

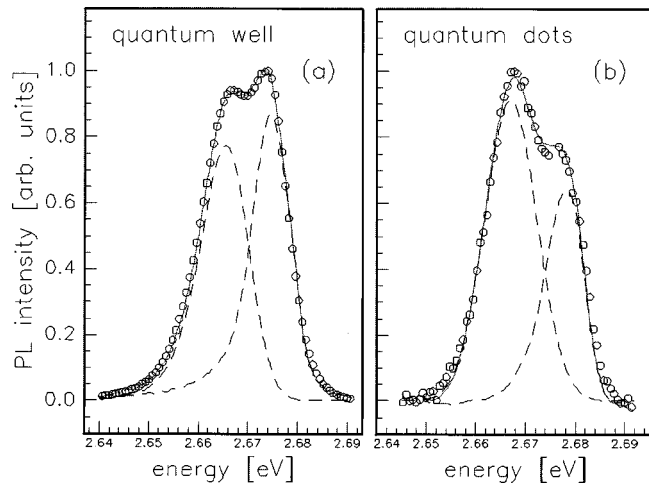


FIG. 3. PL spectra of the unpatterned quantum well (a) for $P = 100 \text{ W/cm}^2$ and of a 35 nm dot array (b) for $P = 50 \text{ W/cm}^2$. The exciton spectrum obtained at low densities (1 W/cm^2), and the biexciton contribution to the line shape as described in the text, are shown as dashed lines.

the QW should even be more appropriate than the usage of a thermal biexciton distribution. With this kind of line shape analysis, a BBE of 8.4 meV is obtained in the QW.

To describe the biexciton line shape of the QD spectra, the quasi-zero-dimensional density of states has to be taken into account. For 35-nm QD's we can neglect higher excited dot states, which are shifted at least 8 meV to higher energies with respect to the ground state, and therefore do not contribute significantly to the PL signal. This can be shown by calculating the energetic distance between the ground state and the excited dot states using the effective-mass

approximation.¹⁷ Thus a single Gaussian function is used to describe the dot ground state. In Fig. 3(b) we plot the model line shape and the experimental data for QD's for an excitation density of 50 W/cm^2 . For comparison, the contributions of biexcitons and excitons are also shown. The experimental data are described rather good using a BBE of 11.3 meV.

As indicated by the evaluation of our data, the BBE is significantly enhanced in QD's compared to the QW, although the lateral extension of the dot is larger than the exciton diameter. This is in agreement with theoretical calculations of Takagahara,⁷ who demonstrated a strong influence of the dielectric confinement on the BBE, which further enhances the BBE in deep-etched QD's as compared to buried ones.

In conclusion, we compared the biexciton formation process and the biexciton binding energy in QD's with a lateral extension of $L_x = 35 \text{ nm}$ and a QW reference by time-resolved PL spectroscopy. The biexciton formation coefficient C was determined by modeling the onset of the biexciton PL signal using a system of rate equations. A strong enhancement of C was found increasing from $C = 0.2 \times 10^{-10} \text{ cm}^2/\text{ps}$ in the case of the QW to $C = 4 \times 10^{-10} \text{ cm}^2/\text{ps}$ for the QD's, indicating a more efficient formation of biexcitons in totally confined II-VI nanostructures. By analyzing the luminescence spectra, a significant increase of the BBE in QD's as compared to the QW reference is found. This is attributed to an increased carrier and dielectric confinement in QD's.

We would like to thank O. Breitwieser for technical assistance in realizing the QD structures, and gratefully acknowledge the financial support of this work by the Deutsche Forschungsgemeinschaft (SFB410).

*Present address: Institut für Festkörperphysik, Universität Bremen, P.O. Box 330440, D-28334 Bremen, Germany.

¹D. Birkedal, J. Singh, V. G. Lyssenko, J. Erland, and J. M. Hvam, *Phys. Rev. Lett.* **76**, 672 (1996).

²F. Kreller, M. Lowisch, J. Puls, and F. Henneberger, *Phys. Rev. Lett.* **75**, 2420 (1995).

³R. Spiegel, G. Bacher, A. Forchel, B. Jobst, D. Hommel, and G. Landwehr, *Phys. Rev. B* **55**, 9866 (1997).

⁴J. Puls, V. V. Rossin, F. Kreller, H. J. Wünsche, St. Renisch, N. Hoffmann, M. Rabe, and F. Henneberger, *J. Cryst. Growth* **159**, 784 (1996).

⁵D. J. Lovering, R. T. Phillips, G. J. Denton, and G. W. Smith, *Phys. Rev. Lett.* **68**, 1880 (1992).

⁶R. C. Miller, D. A. Kleinman, A. C. Gossard, and O. Munteanu, *Phys. Rev. B* **25**, 6545 (1982).

⁷T. Takagahara, *Phys. Rev. B* **39**, 10 206 (1989).

⁸Garnett W. Bryant, *Phys. Rev. B* **41**, 1243 (1990).

⁹K. Brunner, G. Abstreiter, G. Böhm, G. Tränkle, and G. Weimann, *Phys. Rev. Lett.* **73**, 1138 (1994).

¹⁰U. Woggon, O. Wind, W. Langbein, O. Gogolin, and C. Klingshirn, *J. Lumin.* **59**, 135 (1994).

¹¹S. Yano, T. Goto, T. Itoh, and A. Kasuya, *Phys. Rev. B* **55**, 1667 (1997).

¹²Y. Z. Hu, S. W. Koch, M. Lindberg, N. Peyghambarian, E. L. Pollock, and Farid F. Abraham, *Phys. Rev. Lett.* **64**, 1805 (1990).

¹³R. T. Phillips, D. J. Lovering, G. J. Denton, and G. W. Smith, *Phys. Rev. B* **45**, 4308 (1992).

¹⁴M. Illing, G. Bacher, T. Kümmell, A. Forchel, T. Anderson, D. Hommel, B. Jobst, and G. Landwehr, *Appl. Phys. Lett.* **67**, 124 (1995).

¹⁵R. Spiegel, G. Bacher, O. Breitwieser, A. Forchel, B. Jobst, D. Hommel, and G. Landwehr, *Superlattices Microstruct.* **20**, 1252 (1996); G. Bacher, R. Spiegel, T. Kümmell, O. Breitwieser, A. Forchel, B. Jobst, D. Hommel, and G. Landwehr, *Phys. Rev. B* **56**, 6868 (1997).

¹⁶J. C. Kim, D. R. Wake, and J. P. Wolfe, *Phys. Rev. B* **50**, 15 099 (1994).

¹⁷A. Forchel, R. Steffen, M. Michel, A. Pecher, and T. L. Reinecke, in *Proceedings of the 23rd International Conference on the Physics of Semiconductors*, Berlin, edited by M. Scheffler and R. Zimmermann (World Scientific, Singapore, 1996), Vol. 2, p. 1285.